



Dual approach for the colorimetric determination of unamplified microRNAs by using citrate capped gold nanoparticles

Ahmed Ibrahim Nossier¹ · Hana Abdelzaher² · Marwa Matboli³ · Sanaa Eissa^{3,4}

Received: 10 December 2017 / Accepted: 10 March 2018 / Published online: 22 March 2018
© Springer-Verlag GmbH Austria, part of Springer Nature 2018

Abstract

The authors describe a method for the colorimetric determination of unamplified microRNA. It is based on the use of citrate-capped gold nanoparticles (AuNPs) and, alternatively, a microRNA-probe hybrid or a magnetically extracted microRNA that serve as stabilizers against the salt-induced aggregation of AuNPs. The absorbance ratios A_{525}/A_{625} of the reacted AuNP solutions were used to quantify the amount of microRNA. The assay works in the range of 5–25 pmol microRNA. The lower limit of detection (LOD) is 10 pmol. The performance of the method was tested by detection of microRNA-210-3p in totally extracted urinary microRNA from normal, benign, and bladder cancer subjects. The sensitivity and specificity for qualitative detection of urinary microRNA-210-3p using the assay are 74% and 88% respectively, which is consistent with real time PCR based assays. The assay was applied to the determination of specific microRNA by using its specific oligo targeter or following magnetic isolation of the desired microRNA. The method is simple, cost-efficient, has a short turn-around time and requires minimal equipment and personnel.

Keywords MicroRNA-210-3p · MicroRNA detection · Bladder cancer · AuNPs · Magnetic nanoparticles · Salt-induced aggregation · Oligonucleotide adsorption · Oligotargeter · Streptavidin

Introduction

MicroRNAs are short single-stranded noncoding RNAs of about 18–24 nucleotides in length and naturally occurring in eukaryotic cells [1]. MicroRNAs function in RNA silencing

and post-transcriptional regulation of gene expression [2]. The deregulation of their expression has been heavily implicated in several diseases including several cancers [3], kidney disease [4] and cardiac illnesses [5]. These RNA molecules have been widely studied and strongly correlated with patient diagnosis, prognosis and even response to treatment [6]. Playing such critical roles, microRNAs have continuously proven to carry immense diagnostic potential and have often displayed high sensitivity and specificity [7]. Their stability and ease of isolation either from tissues or body fluids enhance their use as diagnostic biomarkers [8].

Detecting microRNAs is challenging due to their extremely small size, low cellular concentration and as being highly homologous [9]. Methods employed to detect miRNAs include quantitative RT-PCR, microarrays and northern blotting. Such traditional techniques present several challenges such as the fact that they are labor-intensive, require highly-trained professionals and sophisticated equipment, have long turn-around times and are incredibly difficult to carry out in a resource-limited setting [10]. Because of these limitations; the development of highly sensitive and cost-effective detection methods is significant and essential. Various methods have been developed, such as nanoparticle-derived probes

Electronic supplementary material The online version of this article (<https://doi.org/10.1007/s00604-018-2767-9>) contains supplementary material, which is available to authorized users.

✉ Ahmed Ibrahim Nossier
ahmednossier@hotmail.com

✉ Sanaa Eissa
drsanaa_mohamed@med.asu.edu.eg

¹ Biochemistry Department, Faculty of Pharmacy, Misr University for Science and Technology (MUST), 6th October City, Giza, Egypt

² Faculty of Biotechnology, October University for Modern Sciences & Arts, 6th October City, Cairo, Egypt

³ Oncology Diagnostic Unit, Medical Biochemistry & Molecular Biology Department, Faculty of Medicine, Ain Shams University, Cairo, Egypt

⁴ Faculty of Medicine Ain Shams Research Institute (MASRI), Cairo, Egypt

[11], isothermal amplification [12], electrochemical methods [13], and more. A common theme of these recently developed methods is the combination of multistep signal amplification with some sensitive signal output unit to achieve good detection efficiency [14].

Gold nanoparticles (AuNPs) display several favorable characteristics making them highly attractive for use in diagnostic assays [15]. The unique optical properties of AuNPs are due to distinctive phenomenon known as surface plasmon resonance (SPR) that depends on the AuNP size and the inter-particle distance [16]. In colloidal solution, this SPR is responsible for the intense colors and high extinction coefficient of AuNPs compared to conventional dyes [17]. Due to these exclusive optical properties, AuNPs have been employed in developing many colorimetric assays for detection of different biological molecules as nucleic acids [18], enzymes [19] and proteins [20].

Several methods for the detection of nucleic acids have been developed which depend, at heart, on the observable color change produced upon the aggregation of AuNPs. These include the cross-linking method, the non-cross-linking method and the use of citrate-capped AuNPs [21].

The method which entails the use of citrate-capped AuNPs relies on the differences in the electrostatic properties of single-stranded and double-stranded nucleic acid molecules. Li and Rothberg have observed that single stranded (ss) - but not double stranded (ds)-oligonucleotides can adsorb on the negatively charged surface of AuNPs. The adsorption rate is sequence length dependent [22, 23]. In contrast, Farkhari et al. 2016 reported that also ds-oligonucleotides can be adsorbed on AuNPs and stabilize them. The ionic strength is the key parameter in determining the stabilizing effect of both single and double stranded oligonucleotides on AuNPs [24].

Based on these previously mentioned observations, we used citrate-capped AuNPs to directly detect microRNAs in a dual approach assay. In the first approach (Fig. 1), hybrid of microRNA molecules with its specific short probe (15 oligonucleotides in length) were used as stabilizers for AuNPs against salt induced-aggregation. In the second approach (Fig. 2), magnetic nanoparticles modified with specific probe will be used to extract specific microRNA. Extracted microRNA molecules can stabilize AuNPs against salt induced-aggregation (Fig. 2b). The aim was to develop a simple, cost-efficient and PCR-free assay for direct determination of microRNA.

Experimental

Materials

Hydrogen tetrachloroaurate (III) (99.99%, $\text{HAuCl}_4 \cdot 3\text{H}_2\text{O}$), tri- sodium citrate, sodium hydroxide and sodium chloride were all purchased from Sigma- Aldrich (St. Louis, MO,

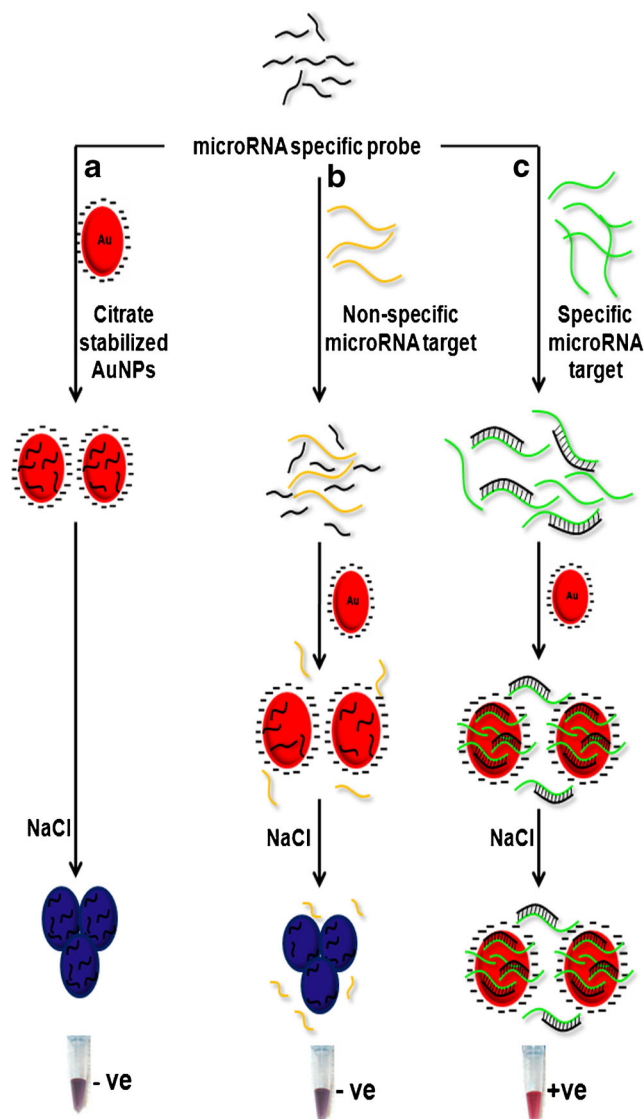


Fig. 1 The principle of the first approach for AuNP-based colorimetric determination of microRNA using specific probe. Matched microRNA hybridizes with its specific probe can stabilize gold nanoparticles (AuNPs) against salt induced aggregation and keeps the red color of AuNPs unchanged

<https://www.sigmaaldrich.com/>). Dynabeads M- 270 Streptavidin was purchased from Invitrogen (Thermo Fisher Scientific Inc.USA, <https://www.thermofisher.com/us/en/home/brands/invitrogen.html>). *Homo sapiens* microRNA-210-3p (has-miR-210-3p) and has-miR-34a mimics (catalogue no:MSY0000267, MSY0000255) and all DNA probes were purchased from Qiagen (Germany, <https://www.qiagen.com/us/>). Sequences of the DNA probes and microRNAs are listed in Table S1 and Table S2. All chemicals were of analytical grade, and all aqueous solutions were prepared with doubly distilled water. The used glassware was cleaned by freshly prepared aqua regia, rinsed thoroughly in doubly distilled water, and dried prior to use.

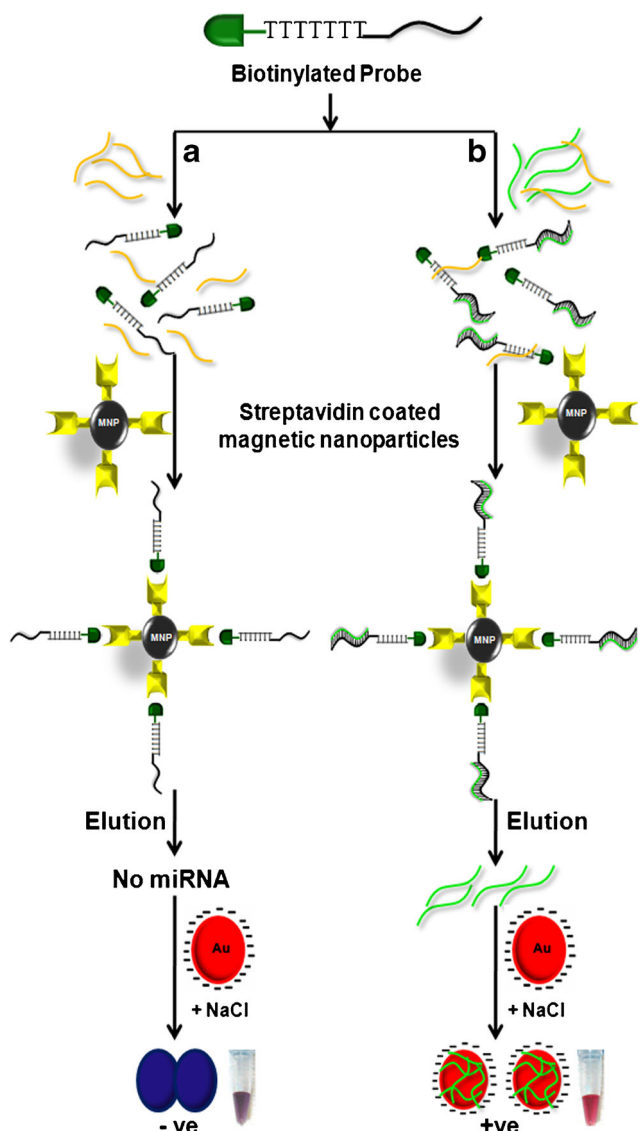


Fig. 2 The principle of the second approach for AuNP-based colorimetric determination of microRNA. Magnetically extracted microRNA can stabilize AuNPs against salt induced aggregation

Clinical samples collection

Samples collection was done following ethical approval by the Medical Ethical Committee of Ain Shams University, Faculty of Medicine, and informed written consent was obtained from each subject ($n = 56$). After cystoscopy and based on histopathologic examination, 31 patients were diagnosed as bladder cancer and 15 were diagnosed as benign urological lesions (see in [Supplementary Material](#)).

Synthesis and characterization of citrate-capped AuNPs

AuNPs were synthesized as reported previously [25] where tri-sodium citrate was used as a reducing and capping agent

(see in [Supplementary Material](#)). The AuNPs were characterized using transmission electron microscopy (TEM) (Model: JEOL-1010, Tokyo, Japan, <https://www.jeol.co.jp/en/>) and dynamic light scattering (DLS) using Malvern zeta-sizer 3000 (Malvern instruments Ltd, UK, <https://www.malvern.com/en>). The λ_{\max} for AuNPs was measured using UV-vis spectrophotometer (Shimadzu UV-1650PC, Tokyo, Japan, <https://www.shimadzu.com/>).

Colorimetric AuNP assay for detection of specific microRNA using specific oligotargeter

In the first approach described, microRNA detection depends on using specific oligotargeter. MicroRNA-210-3p which is reported as potential urinary tumor marker in bladder carcinoma [26] was used as a specific target, while microRNA-34a was used as non-specific target (Table S2). Qiagen probe (Table S1) was used as a specific oligotargeter for microRNA-210-3p. Different salt and oligotargeter concentrations were tested to optimize the assay. The assay was performed as follows: 1 μL of microRNA of varying concentrations were mixed with 1.5 μL hybridization buffer (20 mM phosphate buffer and 1 M NaCl; pH = 7) and 1 μL (10 pmol) of oligotargeter in a final reaction volume of 10 μL . The mixtures were denatured at 95 $^{\circ}\text{C}$ for 30s and annealed at 55 $^{\circ}\text{C}$ for 1 min then cooled to room temperature. 20 μL of colloidal AuNPs were then added to the mixture, and the color was observed with the bare eye (final concentration of NaCl after addition of AuNPs was 50 mM).

To determine the limit of detection (LOD) of the nano-assay, serial dilutions of microRNA-210-3p were assayed as previously mentioned where their spectral profiles were recorded using UV-vis spectrophotometric analyses, the absorbance ratios at 525 and 625 nm (A_{525} / A_{625}) were calculated. A standard curve was generated by plotting the amount of microRNA against its absorbance ratio.

Determination of microRNA-210-3p in urinary total microRNA extract using AuNP assay

In a pilot study, the application of the nano-assay in determination of microRNA-210-3p in urinary total microRNA extract was evaluated. RNA was extracted from urinary pellet of bladder cancer patients using MiRNeasy isolation kit (Qiagen, Germany) according to manufacturer's protocol and as previously published [27]. RNA quality and concentration was then determined using an Ultraspec 1000, UV-vis spectrophotometer (Amersham Pharmacia Biotech, Cambridge, England) and NanoDrop 2000 (Thermoscientific, USA). 5 μL of RNA extract (about 50 $\text{ng}\cdot\mu\text{L}^{-1}$) was mixed with 1.5 μL hybridization buffer and 1 μL of oligotargeter (10 $\text{pmol}\cdot\mu\text{L}^{-1}$) in a final reaction volume of 10 μL . The assay was completed as previously mentioned.

Urinary microRNA-210-3p determination using real time PCR

1 μg total microRNA was polyadenylated by poly (A) polymerase and reverse transcribed to cDNA using miScript Reverse Transcription Kit (Qiagen, Germany) following the manufacturer's protocol (see in [Supplementary Material](#)).

MicroRNA stabilizing effect on AuNPs

In the second approach, microRNA detection depends on the stabilizing effect of microRNA molecules on AuNPs. The salt tolerance of AuNP solution (without aggregation) was tested in the presence of serial dilutions of microRNA. The experiment was done as previously mentioned but without oligotargeter addition.

Magnetic extraction of specific microRNA

Dynabeads M-270 Streptavidin was used for magnetic extraction of microRNA-210-3p using specific Qiagen biotinylated probe (Table S1). Compatibility of microRNA isolated by streptavidin coated magnetic beads with AuNPs was empirically evaluated. The beads were washed and suspended in 2 \times binding and washing (B&W) buffer (10 mM Tris-HCl (pH 7.5), 1 mM EDTA and 2 M NaCl) according to manufacturer's protocol. 25 μL of Dynabeads (5 μg , μL^{-1}) was mixed with 25 μL of hybrid (equimolar mixture (25 pmol) of the specific biotinylated probe and microRNA-210-3p incubated at 55 $^{\circ}\text{C}$). The mixture was shaken for 15 min at room temperature. Then, the tube was placed on a magnet and the supernatant was removed. Two elution methods were tried; heat denaturation at 95 $^{\circ}\text{C}$ and alkaline denaturation. For alkaline denaturation [28], the beads were firstly washed twice with 1 \times saline-sodium citrate buffer (SSC) buffer (150 mM NaCl, 15 mM sodium citrate, pH = 7). Then, the beads were collected using a magnet and the supernatant was removed after each wash. Separately, the beads were suspended in 10 μL of freshly prepared solutions of 10 mM, 20 mM, 50 mM, 100 mM or 150 mM NaOH buffer for 10 min. The tubes were placed on a magnet until all solutions were clear and the eluted microRNA was transferred to a new tube and mixed with 1.5 μL phosphate buffer saline (10 mM phosphate buffer and 0.5 M NaCl; pH = 7). 20 μL of colloidal AuNPs were then added to the mixture, and the color was observed with the bare eye.

Results and discussion

Synthesis and characterization of AuNPs

Synthesized citrate capped AuNPs were characterized by TEM analysis and DLS. TEM observations and the data

obtained from a zeta-sizer have revealed that the AuNPs were spherical and uniformly dispersed as shown in (Fig. S1). The mean diameter was found to be 33 nm (Fig. S3) with negative zeta-potential value -28.8 mV (Fig. S4). The absorption spectrum of the AuNPs exhibited a single peak in the visible region with λ_{max} at 525 nm (Fig. S2). Molar concentration of AuNPs was calculated to be 0.9 nM with $\sim 4.9 \times 10^{11}$ nanoparticles per ml (see in [supplementary material](#)). The absorbance of the AuNP solution was matched to 0.9 at 525 nm.

AuNP assay for determination of specific microRNA

Many biosensors have been developed based on the SPR phenomenon of AuNPs. The presence of target molecules can be detected according to their behaviours with AuNPs. Some target molecules enhance the resistance of AuNPs to aggregate while the others accelerate the aggregation tendency of the AuNPs [29, 30]. Herein, microRNAs detection depends on the stabilizing effect that microRNA molecules provide to AuNPs against salt-induced aggregation.

Adsorption characteristics and the stabilizing effect of both single stranded (ss) - and double stranded (ds) - oligonucleotides on the negatively charged AuNPs may at first seem contradictory. Many previous studies have reported that (ss) - but not (ds) - oligonucleotides can be adsorbed on the AuNPs [22, 23, 31]. While, in these results and in previous study conducted by [24] a remarkable adsorption of ds-oligonucleotides on the AuNPs was found. In order to unravel this conflict certain points should be considered; the first is the length of oligonucleotide. Adsorption and consequently the stabilizing effect of oligonucleotides on AuNPs appear to be sequence length dependent. Both (ss) - and (ds) - oligonucleotides of about 18–24 oligonucleotides in length can rapidly adsorb on the surface of AuNPs. This adsorption increases the surface charge density and stabilizes AuNPs against salt-induced aggregation by enhancing electrostatic repulsion between particles. For the same mole number, the short strands (15 oligonucleotides in length or less) cannot stabilize AuNPs because they do not have enough charges. While, long single or double strands cannot stabilize AuNPs due to their slow adsorption rate resulting from their complicated secondary structure.

The second is the adsorption mechanism. Single stranded oligonucleotides can be adsorbed on AuNPs due to both electrostatic and hydrophobic interactions (electrostatic adsorption between positively charged nitrogenous bases and negatively charged citrate coat of AuNPs). While for ds-oligonucleotides, the distinct adsorption to the AuNPs is owing to chemical interactions between various bases of oligonucleotides with AuNPs. The interaction mechanism seems to be Van der Waals forces between some electronegative atoms in the oligonucleotides and the AuNPs, which have lots of electrons in their valance band. These chemical interactions are very important in determining the stabilizing effect of ds-

oligonucleotides [24]. The difference in adsorption mechanism between (ss) – and (ds) oligonucleotides may explain why the adsorption of ds-oligonucleotides on AuNPs is more sensitive to salt concentration than the adsorption of ss-oligonucleotides.

Optimization of AuNP-assay

For excellent performance of the nano-assay, the concentration of AuNPs, probe and salt were optimized. The salt concentration was critical for detection of specific microRNA. The salt concentration was kept at a minimum threshold (50 mM per final reaction volume) that allows the aggregation of AuNPs in the presence of short probe molecules alone but without disrupts the stabilizing effect of the hybrid (microRNA+ probe) on AuNPs (Fig. S5, S6).

Determination of specific microRNA using specific oligotargeter

The results shown that the assay can be used as a tool for the determination of specific microRNA using its specific oligotargeter. The performance of the assay was evaluated by detecting microRNA-210-3p. While to evaluate the specificity, microRNA-34a was used as non-specific target. In the presence of microRNA-210-3p (specific target), the test color remained red due to adsorption of microRNA-probe hybrid on the AuNPs surface, thus keeping dispersion of AuNPs and prevents salt-induced aggregation. While for non specific target (microRNA-34a), since the probe molecules are being shorter in length than the non-specific microRNA molecules, it will preferentially adsorb to the surface of AuNPs faster than the non-specific microRNA molecules preventing its adsorption to the AuNPs. The test color changed to blue because the short probe molecules adsorbed on AuNPs surface do not stabilize them against salt-induced aggregation (Fig. S7). Serial dilutions of microRNA-210-3p in the range of 0 to 35 pmol were used to determine the limit of detection (LOD) of the assay. The assay works linearly in the range of 5–25 pmol. By visual detection, the lower LOD was found to be 10 pmol (Fig. 3a).

The λ_{\max} of AuNPs was initially located at 525 nm. Salt induce AuNPs aggregation with shift in λ_{\max} to a higher wavelength (red shift). The absorbance at 525 nm decreased and the absorbance at 625 nm increased. MicroRNA-210 molecules hybridize with its specific probe. This hybrid prevented AuNPs aggregation maintaining higher absorbance at 525 nm and lower absorbance at 625 nm. The colorimetric response and the wavelength change are displayed in (Fig. 3b).

The analytical performance of the proposed nano-assay is compared with the previously reported optical methods in Table 1 [32–38]. The LOD of the nano-assay suggested in

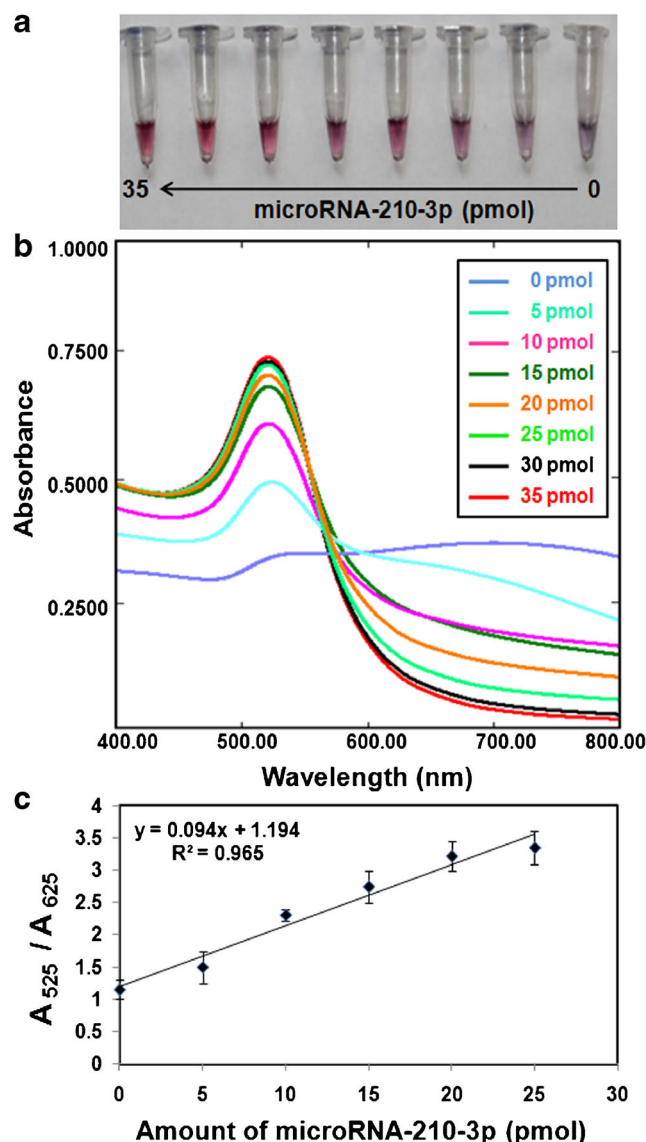


Fig. 3 AuNP-based colorimetric assay for determination of microRNA-210-3p using specific probe. **a** Serial dilutions of microRNA-210-3p in the range of 0 to 35 pmol were prepared to determine the limit of detection (LOD) of AuNP assay. Using this colorimetric method the lower LOD was found to be 10 pmol. **b** Absorption spectra of reacted AuNP solutions in the presence of microRNA-210-3p in the range of 0 to 35 pmol. **c** A plot of spectral absorbance ratios A_{525}/A_{625} of the reacted AuNP solutions as a function of the corresponding amount of microRNA-210-3p. A linear correlation was found between the values of A_{525}/A_{625} and the amount of microRNA-210-3p over the range of 5–25 pmol ($R^2 = 0.965$). Each point represents the mean \pm SD

this work was also comparable to those of other optical methods except of fluorescence based methods. However, narrow linear range was obtained that may be due to dependence of the assay only on the physical adsorption of oligonucleotides on AuNPs to induce a signal. The main advantage of this assay is no complicated experimental steps (such as labeling, immobilization and enzyme amplification) are required.

Table 1 Comparisons of other reported optical methods for miRNA detection

Method applied	Materials used	Linear range	LOD	Ref.
Fluorescence	Graphene oxide – FAM labeled DNA probe – Polymerase	1 f. – 100 nM	0.75fM	[32]
Fluorescence	DNA polymerase – DNA ligase – Nicking enzyme SYBR Green	1 f. – 50 pM	1 fM	[33]
Colorimetric assay	AuNPs – Duplex-specific nuclease – ssDNA probe	10 fmol – 4 pmol	10 fmol	[34]
Colorimetric assay	Capture DNA probe - Hairpin probe – T7exonuclease – Hemin	10 pM – 100 nM	0.69 pM	[35]
Surface Plasmon resonance	SPRi system – AuNPs – Polymerase – Molecular beacon – DNA probe	50 pM – 5 nM	45 pM	[36]
Fluorescence	DNA probe – Copper nanoclusters (CuNC)	50 pM – 10 nM	11 pM	[37]
Colorimetric assay	DNA modified magnetic beads – based on strand displacement strategy	5 nM – 500 nM	3.8 nM	[38]
Colorimetric assay	AuNPs – DNA probe – MNP	5 pmol – 25 pmol	10 pmol	This work

Quantification of microRNA-210-3p

AuNP assay allows quantitative estimation of microRNA-210-3p. The change in assay color intensity was directly proportional to the amount of microRNA used. A series of dilutions of microRNA-210-3p were prepared and the ratios of spectral absorbance A_{525}/A_{625} of their reacted AuNP solutions were plotted as a function of the amount of microRNA (pmol). These two absorbances, A_{525} and A_{625} were chosen to represent the relative amount of non-aggregated and aggregated AuNPs respectively. Figure 3c shows the plot of the values of A_{525}/A_{625} of AuNPs against the amount of microRNA-210 (pmol) and a linear correlation was found ($y = 0.094x + 1.194$, $R^2 = 0.965$).

Qualitative detection of microRNA-210-3p in urinary total microRNA extracts

The applicability of the AuNP-assay for detection of microRNA in clinical sample was evaluated by detection of microRNA-210-3p in totally extracted urinary microRNA from normal, benign and bladder cancer subjects (Fig. 4a). 23 malignant samples out of 31 were positive, with a sensitivity of 74.2%. On the other hand, 9 normal samples out of 10 samples were negative, while 13 benign samples out of 15 were negative and 3 samples were false positive. The specificity of the nano-assay was 88%. These results were consistent with that of the real time RT-PCR for detection of urinary microRNA-210-3p where the sensitivity and the specificity of real time RT-PCR were 71.3% and 91.1 respectively. Difficult quantification of microRNA in real sample is the main limitation of this approach. However, the AuNP assay is cost effective, has short turnaround time (20 min) compared to real time RT-PCR (4 h) and requires minimal equipment and personnel. Figure 5 shows a comparison between the nano-assay and real time RT-PCR.

Detection of specific microRNA following magnetic extraction

The second approach for the detection of unamplified miRNA using citrate-capped AuNPs involved the use of Dynabeads

coupled with a biotinylated probe specific to the target microRNA. The design of the assay entailed two phases: a preliminary phase in which the target microRNA was isolated using the magnetic Dynabeads coupled with a biotinylated probe. A second detection phase in which the unbiotinylated strand was isolated and detected using AuNPs. This approach was believed to enhance the sensitivity and the specificity of the assay and allows quantification of microRNA in real sample due to the prior isolation of the microRNA.

To ensure that microRNA alone would have the capacity to stabilize AuNPs; the salt tolerance of AuNP solution in the presence of microRNA was tested. No color change was observed for AuNP solution in the presence of microRNA and NaCl (50 mM in the final reaction volume) indicating that microRNA molecules can stabilize AuNPs. The LOD was 10 pmol (Fig. 4b).

Next, the assay was implemented by first binding the biotinylated hybrid to the Dynabeads. The biotinylated probe-coated beads were used as a negative control. The unbiotinylated strand was eluted in RNase-free water by brief incubation at 95 °C for 1 min. The eluted solutions were added to the AuNPs, however, an immediate color change was observed using both microRNA and bead-only solutions. This was attributed to the carryover of salt from the B&W buffer. By substituting the B&W buffer with RNase-free water, it was found that no color change occurred even after the addition of salt in both microRNA-containing and microRNA-free eluted solutions. This signified that the eluted solutions stabilize the AuNPs. It was concluded that the brief heating at 95 °C may break streptavidin-biotin bond.

Upon resorting to the manufacturer's website, the use of SSC buffer to wash the beads followed by their incubation in 0.15 M NaOH was recommended. However, this approach gave the same results (full stabilization of AuNPs both with and without the use of the microRNA). Furthermore, to determine the exact reason of the stabilization of the AuNPs, this approach was performed on beads that had not been coupled to the biotinylated probe and the eluted solution was found to stabilize the AuNPs. In light of this new finding, it became clear that the use of SSC buffer and NaOH not only caused the

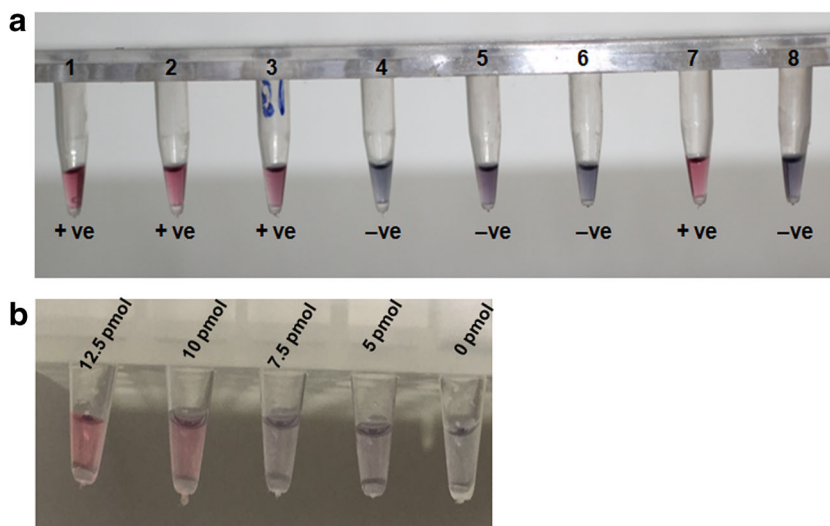


Fig. 4 AuNPs-based colorimetric assay for detection of microRNA-210-3p. **a** Colorimetric AuNP assay for detection of urinary miR-210-3p using specific probe. Positive reaction is shown in the positive control (microRNA-210-3p mimic) (7) and malignant samples (1, 2 and 3), while negative reaction is shown in negative control (blank) (8), benign samples

(4 and 5) and normal sample (6). **b** Salt tolerance of AuNP solutions in the presence of serial dilutions of microRNA-210-3p. No color change was observed for AuNP solution in the presence of microRNA -210-3p (LOD was 10 pmol)

dissociation of biotinylated probe from the beads, it also caused the release of the streptavidin molecules from the surface of the beads.

This hypothesis was confirmed by [28] who had previously reported that the use of NaOH causes the liberation of the streptavidin molecules from the surface of magnetic beads (Dynabeads and Sera-Mag). They detected the presence of the streptavidin in the eluted solution by western blotting using anti-streptavidin antibodies. However, they suggested the use of NaOH alone for alkaline denaturation at the much lower concentration of 10–20 mM to elute the unbiotinylated strand. Trace amounts of streptavidin were detected when such low concentrations were used. Thus, the assay was tested using both 10 mM and 20 mM NaOH concentrations and the AuNPs were found, once more, to be stabilized by the eluted solutions.

The undesired elution of streptavidin when trying to elute unbiotinylated DNA/RNA from streptavidin-coated beads

either using heat, SSC or NaOH is most certainly an issue. This recurrent theme can be observed in numerous studies including those performed by [39–41]. These studies all demonstrate the issues of using streptavidin-coated Dynabeads for the isolation of single-stranded nucleic acids during the generation of aptamers as the release of streptavidin may lead to the formation of undesired streptavidin-specific aptamers during SELEX. The same issues occur when Dynabeads are used for the preparation of ssDNA/RNA for use with AuNPs as the traces of streptavidin can lead to the stabilization of the AuNPs.

It is therefore evident that the use of streptavidin coated magnetic beads for the isolation of microRNA for its subsequent detection using AuNPs is a highly inefficient approach. We recommend that other approaches for the specific isolation of the target microRNA using magnetic nanoparticles be evaluated as this proposed assay is a highly promising one and we are currently investigating the use of thiol-modified probe

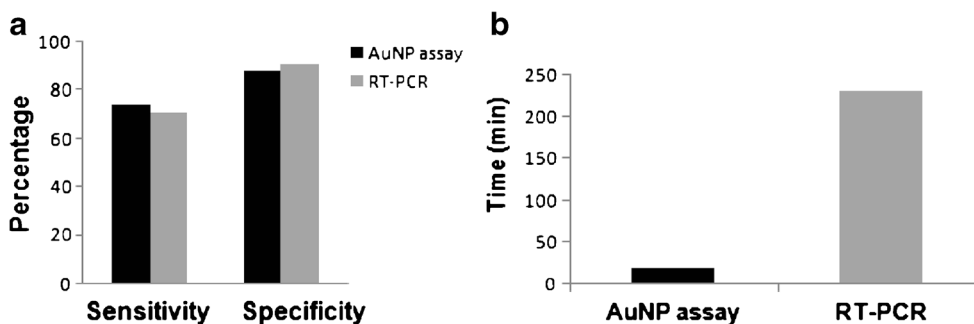


Fig. 5 Comparison between AuNP-assay and real time RT-PCR for determination of urinary microRNA-210-3p. **a** The AuNP-assay showed sensitivity and specificity of 74.2% and 88%, while real time RT-PCR

showed 71.3% sensitivity and 91.1% specificity respectively. **b** The AuNP-assay has short turnaround time (20 min) compared to real time RT-PCR (4 h)

covalently bound to magnetic nanoparticles for this purpose. We believe that, once properly implemented, the use of the preliminary isolation phase will greatly increase the sensitivity and specificity of the assay.

Conclusions

The study at hand involved the development of a dual approach for the detection of unamplified miRNA using citrate-capped gold nanoparticles. The nano-assay utilizing a specific oligotargeter showed great success with a lower LOD of 10 pmol. Results are consistent with qPCR when tested in a pilot study for qualitative detection of miRNA-210-3p in total urinary miRNA extracts. Difficult quantification of microRNA in real sample is the main limitation of this approach. The second approach showed immense potential. However, it was challenged by the inadequacy of streptavidin-coated beads for this intended application. Hence, we are currently investigating the use of thiol-modified probe covalently bound to magnetic nanoparticles for the isolation of specific microRNA and subsequently detected using the nano-assay. This proposed solution shows great promise and may provide a solution to the hurdle met in the isolation of specific microRNA molecules and allows microRNA quantification in real sample.

Acknowledgements This work was financially supported by the national grant: RSTDF 6635. Authors acknowledge Professor Mohamed Esmat, Prof of urology for provision of clinical samples and patient's data. The National patent application number of this work is 1631/2017.

Compliance with ethical standards The authors declare that they have no competing interests.

References

- Ambros V (2004) The functions of animal microRNAs. *Nature* 431:350–355. <https://doi.org/10.1038/nature02871>
- Krol J, Sobczak K, Wilczynska U, Drath M, Jasinska A, Kaczynska D, Krzyzosiak WJ (2004) Structural features of microRNA (miRNA) precursors and their relevance to miRNA biogenesis and small interfering RNA/short hairpin RNA design. *J Biol Chem* 279:42230–42239. <https://doi.org/10.1074/jbc.M404931200>
- Iorio MV, Croce CM (2017) MicroRNA dysregulation in cancer: diagnostics, monitoring and therapeutics. A comprehensive review. *EMBO Mol Med* 9:582. <https://doi.org/10.15252/emmm.201707779>
- Ben-Dov IZ, Tan YC, Morozov P, Wilson PD, Rennert H, Blumenfeld JD, Tuschl T (2014) Urine microRNA as potential biomarkers of autosomal dominant polycystic kidney disease progression: description of miRNA profiles at baseline. *PLoS One* 9:e86856. <https://doi.org/10.1371/journal.pone.0086856>
- Verjans R, Van Bilsen M, Schroen B (2017) MiRNA Deregulation in Cardiac Aging and Associated Disorders. *Int Rev Cell Mol Biol* 334:207–263. <https://doi.org/10.1016/bs.ircmb.2017.03.004>
- Cheng G (2015) Circulating miRNAs: roles in cancer diagnosis, prognosis and therapy. *Adv Drug Deliv Rev* 81:75–93. <https://doi.org/10.1016/j.addr.2014.09.001>
- Bertoli G, Cava C, Castiglioni I (2015) MicroRNAs: New Biomarkers for Diagnosis, Prognosis, Therapy Prediction and Therapeutic Tools for Breast Cancer. *Theranostics* 5:1122–1143. <https://doi.org/10.7150/thno.11543>
- Wang J, Chen J, Sen S (2016) MicroRNA as Biomarkers and Diagnostics. *J Cell Physiol* 231:25–30. <https://doi.org/10.1002/jcp.25056>
- Leshkowitz D, Horn-Saban S, Parmet Y, Feldmesser E (2013) Differences in microRNA detection levels are technology and sequence dependent. *RNA* 19:527–538. <https://doi.org/10.1261/ma.036475.112>
- Tian T, Wang J, Zhou X (2015) A review: microRNA detection methods. *Org Biomol Chem* 13:2226–2238. <https://doi.org/10.1039/c4ob02104e>
- Hwang DW, Song IC, Lee DS, Kim S (2010) Smart magnetic fluorescent nanoparticle imaging probes to monitor micro RNAs. *Small* 6:81–88. <https://doi.org/10.1002/sml.200901262>
- Li C, Li Z, Jia H, Yan J (2011) One-step ultrasensitive detection of microRNAs with loop-mediated isothermal amplification (LAMP). *Chem Commun* 47:2595–2597. <https://doi.org/10.1039/c0cc03957h>
- Li F, Peng J, Wang J, Tang H, Tan L, Xie Q, Yao S (2014) Carbon nanotube-based label-free electrochemical biosensor for sensitive detection of miRNA-24. *Biosens Bioelectron* 54:158–164. <https://doi.org/10.1016/j.bios.2013.10.061>
- Zhu X, Zhou X, Xing D (2013) Label-free detection of micro-RNA: two-step signal enhancement with a hairpin-probebased graphene fluorescence switch and isothermal amplification. *Chemistry* 19:5487–5494. <https://doi.org/10.1002/chem.201204605>
- Mieszawska AJ, Mulder WJM, Fayad ZA, Cormode DP (2013) Multifunctional gold nanoparticles for diagnosis and therapy of disease. *Mol Pharm* 10:831–847. <https://doi.org/10.1021/mp3005885>
- Rechberger W, Hohenau A, Leitner A, Krenn JR, Lamprecht B, Aussenegg FR (2003) Optical properties of two interacting gold nanoparticles. *Opt Commun* 220:137–141. [https://doi.org/10.1016/S0030-4018\(03\)01357-9](https://doi.org/10.1016/S0030-4018(03)01357-9)
- Huang KS, Lin YC, Su KC, Chen HY (2007) An electroporation microchip system for the transfection of zebrafish embryos using quantum dots and GFP genes for evaluation. *Biomed Microdevices* 9:761–768. <https://doi.org/10.1007/s10544-007-9087-x>
- Liandris E, Gazouli M, Andreadou M, Comor M, Abazovic N, Sechi LA, Ikonomopoulos J (2009) Direct detection of unamplified DNA from pathogenic mycobacteria using DNA-derivatized gold nanoparticles. *J Microbiol Methods* 78:260–264. <https://doi.org/10.1016/j.mimet.2009.06.009>
- Nossier AI, Mohammed OS, Fakhr El-Deen RR, Zaghoul AS, Eissa S (2016) Gelatin-modified Gold Nanoparticles for Direct Detection of Urinary total Gelatinase activity: Diagnostic value in Bladder Cancer. *Talanta* 161:511–519. <https://doi.org/10.1016/j.talanta.2016.09.015>
- Bonomi R, Cazzolaro A, Sansone A, Scrimin P, Prins LJ (2011) Detection of enzyme activity through catalytic signal amplification with functionalized gold nanoparticles. *Angew Chem Int Ed Eng* 50:2307–2312. <https://doi.org/10.1002/anie.201007389>
- He S, Liu DB, Wang Z, Cai KY, Jiang XY (2011) Utilization of unmodified gold nanoparticles in colorimetric detection. *Sci China Phys Mech Astron* 54:1757–1765. <https://doi.org/10.1007/s11433-011-4486-7>
- Li H, Rothberg LJ (2004) Colorimetric detection of DNA sequences based on electrostatic interactions with unmodified gold nanoparticles. *Proc Natl Acad Sci U S A* 101:14036–14039. <https://doi.org/10.1073/pnas.0406115101>

23. Li H, Rothberg LJ (2005) Detection of Specific Sequences in RNA Using Differential Adsorption of Single-Stranded Oligonucleotides on Gold Nanoparticles. *Anal Chem* 77:6229–6233. <https://doi.org/10.1021/ac050921y>
24. Farkhari N, Abbasian S, Moshaii A, Nikkha M (2016) Mechanism of adsorption of single and double stranded DNA on gold and silver nanoparticles: Investigating some important parameters in biosensing applications. *Colloids Surf B: Biointerfaces* 148:657–664. <https://doi.org/10.1016/j.colsurfb.2016.09.022>
25. Hill HD, Mirkin CA (2006) The bio-barcode assay for the detection of protein and nucleic acid targets using DTT-induced ligand exchange. *Nat Protoc* 1:324–336. <https://doi.org/10.1038/nprot.2006.51>
26. Eissa S, Matboli M, Hegazy MG, Kotb YM, Essawy NO (2015) Evaluation of urinary microRNA panel in bladder cancer diagnosis: relation to bilharziasis. *Transl Res* 165:731–739. <https://doi.org/10.1016/j.trsl.2014.12.008>
27. Lorenzen JM, Volkmann I, Fiedler J, Schmidt M, Scheffner I, Haller H, Gwinner W, Thum T (2011) Urinary miR-210 as a mediator of acute T-cell mediated rejection in renal allograft recipients. *Am J Transplant* 11:2221–2227. <https://doi.org/10.1111/j.1600-6143.2011.03679.x>
28. Kilil GK, Tilton L, Karbiwnyk CM (2016) NaOH concentration and streptavidin bead type are key factors for optimal DNA aptamer strand separation and isolation. *BioTechniques* 61:114–116. <https://doi.org/10.2144/000114449>
29. Liu X, Wang Y, Chen P, Wang Y, Zhang J, Aili D, Liedberg B (2014) Biofunctionalized gold nanoparticles for colorimetric sensing of botulinum neurotoxin a light chain. *Anal Chem* 86:2345–2352. <https://doi.org/10.1021/ac402626g>
30. Li ZJ, Zheng XJ, Zhang L, Liang RP, Li ZM, Qiu JD (2015) Label-free colorimetric detection of biothiols utilizing SAM and unmodified Au nanoparticles. *Biosens Bioelectron* 68:668–674. <https://doi.org/10.1016/j.bios.2015.01.062>
31. Nelson EM, Rothberg LJ (2011) Kinetics and mechanism of single-stranded DNA adsorption onto citrate-stabilized gold nanoparticles in colloidal solution. *Langmuir* 27:1770–1777. <https://doi.org/10.1021/la102613f>
32. Li Y, Pu Q, Li J, Zhou L, Tao Y, Li Y, Xie G (2017) An “off-on” fluorescent switch assay for microRNA using nonenzymatic ligation-rolling circle amplification. *Microchim Acta* 184:4323–4330. <https://doi.org/10.1007/s00604-017-2475-x>
33. Zhou Y, Li B, Wang M, Wang J, Yin H, Ai S (2017) Fluorometric determination of microRNA based on strand displacement amplification and rolling circle amplification. *Microchim Acta* 184:4359–4365. <https://doi.org/10.1007/s00604-017-2450-6>
34. Shi HY, Yang L, Zhou XY, Bai J, Gao J, Jia HX, Li QG (2017) A gold nanoparticle-based colorimetric strategy coupled to duplex-specific nuclease signal amplification for the determination of microRNA. *Microchim Acta* 184:525–531. <https://doi.org/10.1007/s00604-016-2030-1>
35. Sang Y, Xu Y, Xu L, Cheng W, Li X, Wu J, Ding S (2017) Colorimetric and visual determination of microRNA via cycling signal amplification using T7 exonuclease. *Microchim Acta* 184(7):2465–2471. <https://doi.org/10.1007/s00604-017-2238-8>
36. Zeng K, Li H, Peng Y (2017) Gold nanoparticle enhanced surface plasmon resonance imaging of microRNA-155 using a functional nucleic acid-based amplification machine. *Microchim Acta*. <https://doi.org/10.1007/s00604-017-2276-2>
37. Borghei YS, Hosseini M, Ganjali MR (2017) Fluorescence based turn-on strategy for determination of microRNA-155 using DNA-templated copper nanoclusters. *Microchim Acta* 184:2671–2677. <https://doi.org/10.1007/s00604-017-2272-6>
38. Ji X, Lv H, Ma M, Lv B, Ding C (2017) An optical DNA logic gate based on strand displacement and magnetic separation, with response to multiple microRNAs in cancer cell lysates. *Microchim Acta* 184(8):2505–2513. <https://doi.org/10.1007/s00604-017-2248-6>
39. Paul A, Avci-Adali M, Ziemer G, Wendel HP (2009) Streptavidin-coated magnetic beads for DNA strand separation implicate a multitude of problems during cell-SELEX. *Oligonucleotides* 19:243–254. <https://doi.org/10.1089/oli.2009.0194>
40. Svobodová M, Pinto A, Nadal P, O’Sullivan CK (2012) Comparison of different methods for generation of single-stranded DNA for SELEX processes. *Anal Bioanal Chem* 404: 835–842. <https://doi.org/10.1007/s00216-012-6183-4>
41. Liang C, Li D, Zhang G, Li H, Shao N, Liang Z, Zhang L, Lu A, Zhang G (2015) Comparison of the methods for generating single-stranded DNA in SELEX. *Analyst* 140:3439–3444. <https://doi.org/10.1039/c5an00244c>